INSTITUTE OF PHYSICS PUBLISHING PLASMA PHYSICS AND CONTROLLED FUSION

Plasma Phys. Control. Fusion **48** (2006) A121–A129 doi:10.1088/0741-3335/48/5A/S11

Comparisons of small ELM H-Mode regimes on the Alcator C-Mod and JFT-2M tokamaks

A E Hubbard[1,4], K Kamiya[2], N Oyama[1], N Basse[1], T Biewer[1], E Edlund[1], J W Hughes[1], L Lin[1], M Porkolab[1], W Rowan[3], J Snipes[1], J Terry[1] and S M Wolfe[1]

[1] MIT Plasma Science and Fusion Center, Cambridge MA, 02139, USA
[2] Japan Atomic Energy Agency, Naka-city, Ibaraki 311-0193, Japan
[3] Fusion Research Center, University of Texas at Austin, TX, USA

E-mail: Hubbard@psfc.mit.edu

Received 18 October 2005, in final form 23 December 2005
Published 19 April 2006
Online at stacks.iop.org/PPCF/48/A121

Abstract

Comparisons of H-mode regimes were carried out on the Alcator C-Mod and JFT-2M tokamaks. Shapes were matched apart from aspect ratio, which is lower on C-Mod. The high recycling steady H-mode on JFT-2M and enhanced D-alpha (EDA) regime on C-Mod, both of which feature very small or no ELMs, are found to have similar access conditions in $q_{95} - \nu^*$ space, occurring for pedestal collisionality $\nu^* \gtrsim 1$. Differences in edge fluctuations were found, with lower frequencies but higher mode numbers on C-Mod. In both tokamaks an attractive regime with small ELMs on top of an enhanced D_α baseline was obtained at moderate ν^* and higher pressure. The JFT-2M shape favoured the appearance of ELMs on C-Mod and also resulted in the appearance of a lower frequency component of the quasicoherent mode during EDA.

(Some figures in this article are in colour only in the electronic version)

1. Introduction

The high confinement or 'H-mode' regime, characterized by an edge transport barrier or 'pedestal', requires some form of edge relaxation mechanism increasing particle transport, so as to control impurities and maintain steady density while maintaining good energy confinement. This is often provided by edge localized modes (ELMs); the Type I ELM regime is obtained on many tokamaks and is the reference scenario for ITER. However, there are concerns about the heat pulses resulting from such large ELMs and their possible impact on divertor erosion [1]. This motivates the exploration of high confinement regimes with smaller or no ELMs. A number of such regimes have been discovered on various tokamaks, as recently

[4] Author to whom any correspondence should be addressed.

reviewed by Oyama [2]. However, understanding of the physics of, the relations between and the access conditions for these regimes is incomplete.

This paper reports on a series of recent experiments aimed at comparing two such regimes, the enhanced D-alpha (EDA) H-mode regime first observed on the Alcator C-Mod tokamak in 1996 [3] and the high recycling steady H-mode seen on the JFT-2M tokamak in 2002 [4]. The EDA regime is characterized by good steady-state energy confinement, with normalized H-mode confinement, $H_{\mathrm{ITER98\text{-}y2}}$ [5], at or above 1.0, comparable to ELM-free H-mode, steady density and low, steady radiation levels [6]. No periodic ELMs are typically seen, though there are clear pedestals in temperature and density. Instead, the plasma particle content is found to be regulated by a continuous 'quasicoherent (QC) mode' located in the density barrier [7–9]. This mode, observed by several diagnostics, has $f \sim 100$ kHz and poloidal wavenumber, $k_\theta \sim 2\,\mathrm{cm}^{-1}$, near the outer midplane. At high plasma pressure, $\beta_\mathrm{N} > 1.3$, the QC mode broadens in frequency and is largely replaced by a series of small ELMs appearing on top of the generally high D_α level [10]. The HRS H-mode shares many of the global characteristics of the EDA regime, with global confinement factors $H_{\mathrm{ITER89\text{-}P}}$ [11] $\leqslant 1.6$ and $H_{\mathrm{ITER98\text{-}y2}}$, which are less precisely known due to uncertainties in fast ion contribution, of ~0.8, both about 20% lower than ELMy H-mode. Studies of edge fluctuations have found both high frequency (HF) components, with $f \sim 200$–350 kHz, $n \sim 8$ and low frequency (LF), broadband fluctuations with $f \sim 50$ kHz, which have $n = 1$ and $m \sim 4$ [12,13]. Under some conditions, a 'mixed' regime with some small ELMs occurs. Both the EDA and HRS regimes are generally favoured by higher target density or neutral pressure and by increased triangularity, δ, and safety factor, q_{95}. It is thus natural to ask whether they in fact represent the same physical phenomenon, and, if so, how this would extrapolate to other devices.

2. Description of experiments

H-mode regimes, stability and fluctuations are known to depend sensitively on shape. To reduce these effects in the intermachine comparison, shapes on JFT-2M and C-Mod were matched in poloidal cross-section, as shown in figure 1. This also shows that the JFT-2M shape is quite different from the more typical C-Mod shape on which prior H-mode studies have been done, notably lower κ (1.49) and increased lower triangularity, $\delta_\mathrm{L} = 0.77$. However, it was not practical to match the aspect ratio, which is higher on JFT-2M ($R/a = 1.29/0.26\,m = 4.9$) than on C-Mod ($R/a = 0.68/0.21\,m = 3.2$); this means that the plasma dimensionless parameters and safety factor profile, $q(r)$, cannot all be matched exactly. B_T was 5.4 T for C-Mod and 1.6–2.2 on JFT-2M.

Experiments were first carried out on JFT-2M using variations in wall fuelling in a boronized vessel to scan density for several $I_\mathrm{p}/B_\mathrm{T}$ combinations, giving q_{95} of 2.9 (315 kA/2.2 T), 3.2–3.5 (210 kA/2.2 T, 260 kA/1.8 T) and 4.8 (315 kA/2.2 T). Heating was provided by 1.4 MW of balanced NBI. Details of the resulting H-mode regimes, pedestal parameters and fluctuations were reported by Kamiya [14]. C-Mod then conducted experiments in the matched shape on several run days in the 2004 and 2005 campaigns, varying both target density and ICRH power (0–5.2 MW of D(H) heating at $f = 80$ MHz) to vary pedestal parameters at each of the above q_{95} values, corresponding to $I_\mathrm{p} = 1.1$, 0.93 and 0.62 MA. The vessel was boronized in most experiments, with some variation in coating thickness. In both tokamaks, boronization was found to be necessary to achieve steady H-modes and to access the EDA or HRS regimes. While the reason for this is not fully understood, recent experiments on C-Mod, which has Molybdenum plasma facing components, indicate that reducing the impurity sources and rate of rise of radiation is important [15]. Changes in recycling may also play a role.

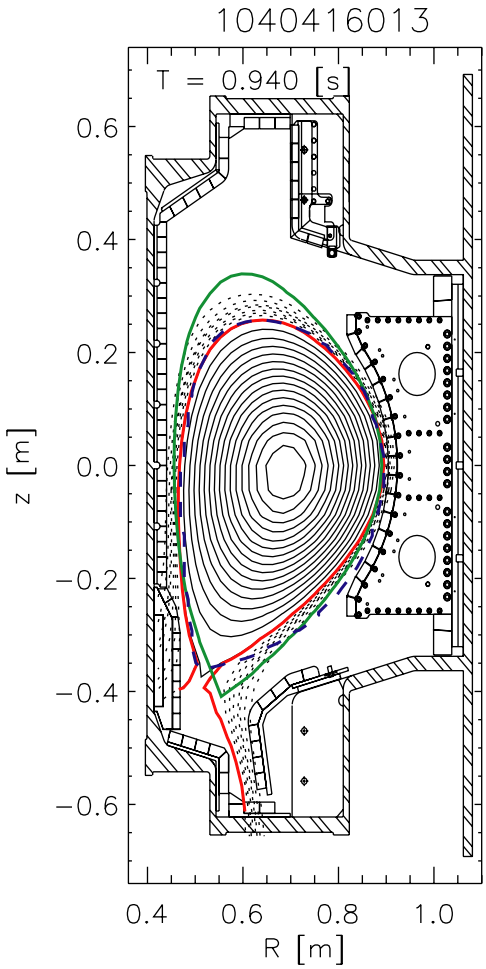

Figure 1. C-Mod shape used in comparison experiments (red) is a good match to scaled JFT-2M shape (blue, dashed) and differs from more typical C-Mod shapes (e.g. green).

3. Results of comparisons

3.1. H-Mode regimes and access conditions

The H-mode regimes obtained span the range of those observed in prior JFT-2M and C-Mod experiments. The pedestal parameter ranges accessed are summarized in figure 2. Figure 2(*a*) shows time trajectories of $T_{\mathrm{e,edge,}}$ versus $T_{\mathrm{e,edge,}}$ for three typical JFT-2M discharges at $q_{95} = 3.5$. Since detailed pedestal profiles were not available, the line averaged density from the outermost chord interferometer at $R = 1.1$ m, typically slightly inboard of the pedestal, was used along with a corresponding ECE channel for T_{e} [14]. Each discharge evolves rapidly after the L-H transition, indicated by the lower curve, and reaches a constant, apparently limiting, pressure curve which it follows as n_{e} rises. At the lowest L-mode target density (blue curve) large ELMs were seen with a baseline D_α level below that of the L-mode. These appear similar to Type I ELMs, though this has not been definitively established, and have the highest pressure limit corresponding to toroidal beta at the pedestal $\beta_{\mathrm{e,ped}} \sim 0.2\%$. At the highest L-mode n_{e}

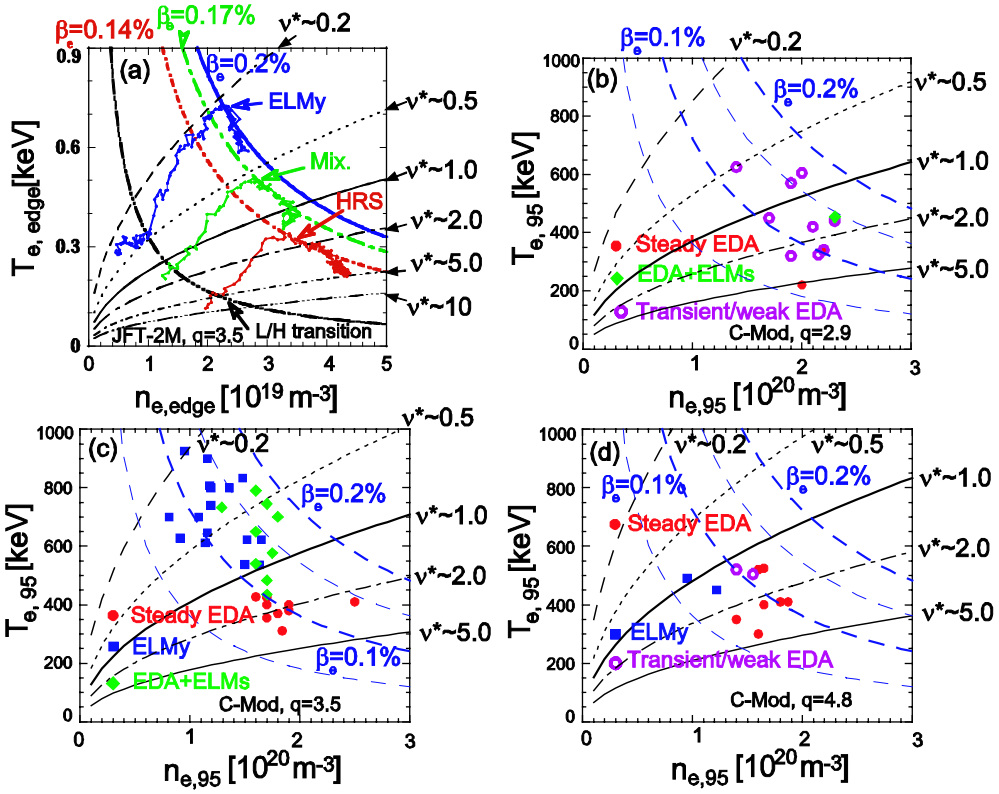

Figure 2. Pedestal T_e and n_e spaces and regimes for (*a*) JFT-2M, $q_{95} = 3.5$, (*b*) C-Mod, $q_{95} = 2.9$, (*c*) C-Mod, $q_{95} = 3.5$ and (*d*) C-Mod, $q_{95} = 4.8$. Lines of constant collisionality ν^*_{ped} and normalized pressure $\beta_{e,ped}$ are drawn for comparison.

(red curve), a steady HRS regime is found with very small ELMs and a D_α level more than twice that of the L-mode. A reduced pressure limit, $\beta_{e,ped} \sim 0.14\%$, is found in this regime. The intermediate regime labelled 'mixed' (green) has more distinct ELMs but still a high D_α level and $\beta_{e,ped} \sim 0.17\%$. All three regimes lead to H-modes with fairly steady density and temperature; the global confinement varies in rough proportion to the pedestal pressure.

On C-Mod, the greatest range of pedestal parameters, and regimes, was achieved in the scans at $q_{95} = 3.5$ (figure 2(*c*)). Because of the variable heating power, a wider range of pressures was accessed in the C-Mod experiments. Detailed edge profiles of n_e and T_e are obtained with Thomson scattering and ECE and confirm a clear transport barrier in all regimes [8, 16]. Edge values were taken at the 95% poloidal flux surface, just inside the pedestal. Pedestal T_i, where measured spectroscopically, was close to the measured T_e, so total β is about twice the $\beta_{e,ped}$ shown. Steady EDA discharges without any discrete ELMs occurred at high densities and modest pressures. At similar densities but higher power and pressures, the small ELM regime with enhanced D_α, labelled 'EDA + ELMs', was obtained as described in [10]. $\beta_{e,ped}$ was up to ~0.17%, comparable to the JFT-2M 'mixed' regime. Atypically for C-Mod, at lower densities regular ELMs were seen in many discharges. Their occurrence was sensitive to shape, as discussed further in section 3.3. Smaller ranges of edge parameters were accessed in the scans at higher and lower q_{95}. At $q_{95} = 2.9$, as has been found previously, steady EDA H-modes could only be achieved at high ν^*. The discharges labelled

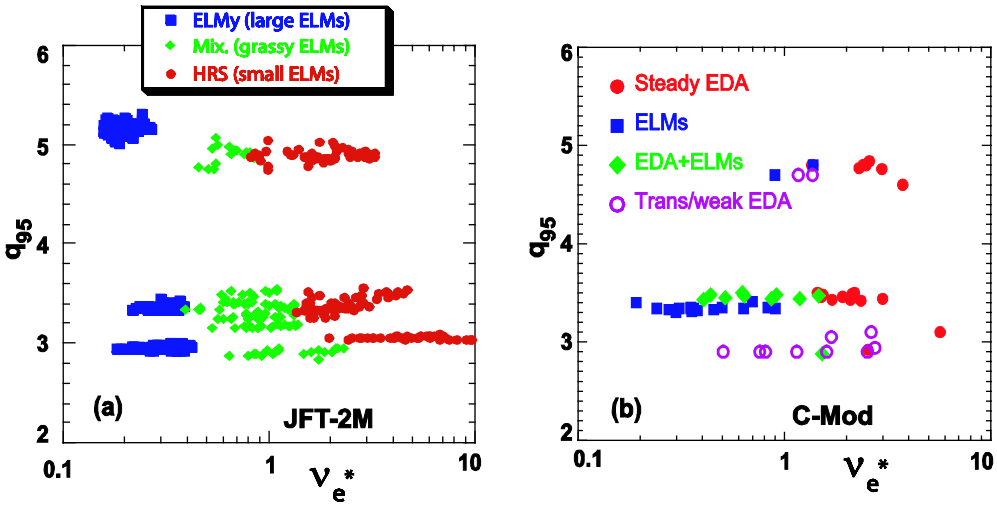

Figure 3. Operational spaces q_{95} versus pedestal ν^* of H-mode regimes on (*a*) JFT-2M and (*b*) C-Mod. Note that the HRS and EDA regimes have similar access conditions, as do the 'Mix' and 'EDA + ELMs' regimes.

'Transient/weak EDA' had a weak QC mode which was insufficient to maintain steady density conditions. Steady EDA was readily obtained at $q_{95} = 4.8$. However, the pressure was limited in these experiments and the high β, small ELM regime was thus not obtained.

Access conditions for regimes on JFT-2M and C-Mod are compared in figure 3, which plots q_{95} versus $\nu^*_{\rm ped}$, defined as the ratio of the collision frequency to the bounce frequency,

$$\nu^*_{\rm e} = 6.921 \times 10^{18} q_{95} R n_{\rm e} Z_{\rm eff} \ln \Lambda / (T_{\rm e}^2 \varepsilon^{3/2}), \quad (1)$$

where $T_{\rm e}$ and $n_{\rm e}$ are evaluated near the top of the pedestal. $Z_{\rm eff} = 1$ is assumed in the ν^* calculation for consistency since measurements were not available in all discharges, so that values are underestimates. A clear separation by ν^* is found on JFT-2M; HRS occurs at highest values, typically > 1.5 and large ELMs at $\nu^* \lesssim 0.5$, with the 'mixed' regime at intermediate ν^*. There is a weak dependence on q_{95}, with the ν^* boundaries shifting to lower values at higher q_{95}. The access conditions on C-Mod are strikingly similar, particularly at $q_{95} = 3.5$. As for HRS, EDA H-modes occur for $\nu^* > 1.5$. Below $\nu^* = 0.4$, only ELMy discharges are seen. There is overlap of ELMy (low D_α) and EDA + ELM (small ELMs, high D_α) H-modes at intermediate ν^*. This may be a result of the wider range of $\beta_{\rm ped}$ in the C-Mod dataset; the latter regime prevails at higher pressure. As has been found in prior experiments, steady EDA H-modes were obtained more easily at $q_{95} \geqslant 3.4$; for $q_{95} = 2.9$ the ν^* boundary increased to $\nu^* > 2$. Weak QC modes were, however, observed at lower ν^*.

3.2. Edge fluctuations in HRS and EDA H-Modes

Since the HRS and EDA regimes are characterized by edge fluctuations thought to cause the enhanced transport, it is of interest to compare these fluctuations under closely matched conditions. Figure 4 shows magnetic fluctuation spectra for two such discharges, both with $q_{95} = 3.4$ and $\nu^*_{\rm ped} = 1.4$. The JFT-2M spectra (*a*) are obtained with probes, described in detail in [13], located near the outer midplane about 11 cm outside the separatrix and feature a HF mode at 340 kHz, with a FWHM of ∼25 kHz. Increased fluctuations are also seen at $f < 100$ kHz. Small ELMs, not shown in the figure, also occur with a period of ∼3 ms, though

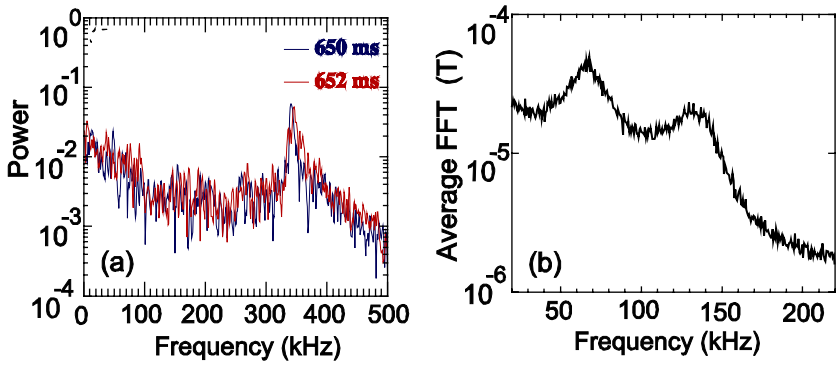

Figure 4. Comparison of magnetic fluctuation spectra measured by probes on (*a*) JFT-2M, during HRS H-mode (*b*) C-Mod, during EDA H-mode with matched shape. Both discharges have $q_{95} = 3.4$ and $\nu^*_{\rm ped} = 1.4$.

the HF and LF modes precede the ELMs and are thought to cause most of the transport [14]. Fluctuations on C-Mod (*b*), which were measured with a magnetic probe head mounted on scanning probe close to the LCFS, show peaks at 134 and 67 kHz. The 134 kHz feature, which appears first in time, is typical of the QC mode reported in standard C-Mod shapes and has $k_{\theta,\rm mid} \sim 2\,{\rm cm}^{-1}$. The lower f peak is a typical and appears to be associated with the JFT-2M shape. It has exactly half the wavenumber as well as frequency, indicating that it occurs on the same rational surface; the lower k probably explains the higher apparent amplitude on magnetics. The two-frequency spectrum is also seen on density fluctuations measured by phase contrast imaging [7], which give slightly higher amplitude for the 134 kHz component. The higher frequency seen on JFT-2M is not expected from dimensional considerations; for identical dimensionless parameters, a higher frequency, $f \sim a^{-5/4}$, would be expected on the smaller, higher field C-Mod device.

Differences are also found in the mode numbers of fluctuations on JFT-2M and C-Mod. On JFT-2M, magnetics arrays show the LF fluctuations have $n = 1$ and $m = 4 \pm 1$. The HF mode has $n = 7$, which, assuming fluctuations at the same location, corresponds to $m \sim 28$. The quasicoherent mode on C-Mod has a wide spectrum of toroidal mode numbers centred at $n \sim 11$ for the 67 kHz component, which corresponds to $n \sim 22$ at 134 kHz. Poloidal wavenumber, k_θ, is measured both from magnetics, just above the outer midplane, and PCI, viewing the top and bottom of the plasma where typically $k_\theta \sim 5\,{\rm cm}^{-1}$, since k_θ varies poloidally as expected. The average poloidal mode numbers corresponding to $k_{\theta,\rm mid}$ of 1 and $2\,{\rm cm}^{-1}$ are computed to be $m \sim 65$ and 130, respectively, for the low and HF components, significantly higher than for JFT-2M.

Interestingly, at $q_{95} = 4.8$, the QC mode on C-Mod became quite weak at high density ($\nu^* \gtrsim 2$), although steady H-modes with enhanced D_α were maintained. In these conditions, broadband density fluctuations at $f < 100$ kHz increased markedly on PCI spectra and probably contributed to particle transport. This behaviour is similar to that of the LF fluctuations in JFT-2M.

3.3. ELM behaviour on C-Mod

As mentioned above, the appearance of a regime of distinct large ELMs, without enhanced D_α, is highly unusual on C-Mod. Figure 5 shows an example of an H-mode with large ELMs, corresponding to one of the lowest collisionality points on figures 2(*c*) and 3(*b*). No QC mode was

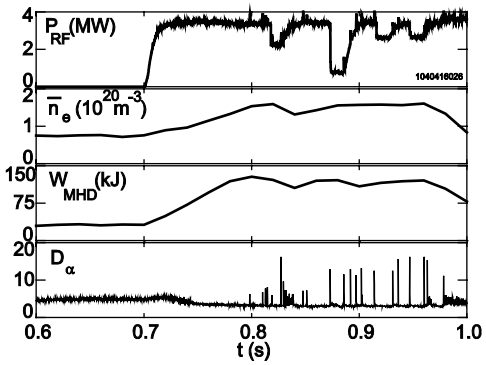

Figure 5. Example of a C-Mod H-mode with low ν^* and large ELMs.

seen, indicating that the ELMs were maintaining the fairly steady density. ELM size was quite variable within and between discharges, with the amplitude of D_α spikes ranging from 0.4 to 2.4 times the L-mode level. The largest ELMs occurred only at lowest ν^*, <0.4. The duration of spikes was also variable, typically 0.5–1.5 ms. Individual ELMs have very small effects (<1%) on the global stored energy and line averaged density, though brief drops in the pedestal temperature (∼10%) are sometimes seen using ECE diagnostics. MHD precursors with decreasing f, ∼200–50 kHz, occurred ∼1 ms before ELMs. Fast D_α diode and 2-D camera measurements also show precursors, as well as extended 'filaments' in the SOL during an ELM [17].

The type, or types, of these ELMs is not yet clear. The largest ELMs occur at pressures close to the highest seen in this set of experiments, and may be Type I ELMs. On the other hand, as seen in figure 2 (blue points), many ELMs (typically of lower amplitude) occurred in the lower pressure and temperature pedestals, clearly below the observed pressure limit. Prior stability analysis of the C-Mod EDA + ELM regime (green), in contrast, found pedestals above the peeling–ballooning stability limit [10]. In some discharges ELMs stopped when a sawtooth heat pulse transiently raised the edge T_e. These observations suggest that they are more likely to be Type III than Type I ELMs, though a definitive MHD identification has not been made.

ELM occurrence was reproducible and highly dependent on shape, with the JFT-2M matching shape shown in figure 1 serendipitously favourable. Low target density $\bar{n}_e \sim 8 \times 10^{19}\,m^{-3}$, close to that of the observed low density limit for accessing H-mode on C-Mod, was required. Further experiments in which the shape was varied show that, when the X-point location was shifted outward by 2–4 cm, ELMs disappeared and were replaced by 'dithering' H-mode, with regular L-mode periods of 5–10 ms. H-modes with large ELMs have been seen in a few other C-Mod experiments, also at low collisionality, in which the plasma was limited, or nearly limited, on the inner 'nose' of the divertor [18]. Both results suggest that the location of the X-point is important for stability, probably due to the increased lower triangularity, $\delta_L \sim 0.79$, as compared with typical C-mod values, $\delta_L < 0.55$. A detailed stability analysis and more systematic scans of shape are required to confirm and understand this sensitivity, as well as to clarify the ELM type and responsible MHD instability.

4. Discussion and conclusions

Comparison experiments between JFT-2M and Alcator C-Mod have provided considerable information on the similarities and differences between H-mode regimes. The similarities in

dimensionless parameters required to access various regimes are striking. Both the EDA and HRS regimes, steady regimes with continuous HF fluctuations, occur for $\nu^*_{\rm ped} \gtrsim 1$, with the exact collisionality boundary weakly depending on q_{95}. The upper bound of $\beta_{\rm e,ped} \sim 0.14\%$ was also comparable, though this was not scanned systematically. The 'mix' regime seen on JFT-2M, with small ELMs on an enhanced D_α baseline, appears quite similar to the C-Mod regime of small ELMs arising from EDA at higher β. For $q_{95} = 3.5$, both occur in these experiments at $0.4 < \nu^*_{\rm ped} < 1.5$ and at $\beta_{\rm e,ped}$ up to 0.17%. These results strongly suggest a correspondence of these regimes. The situation regarding ELMy H-modes is less clear. As on JFT-2M, at $\nu^*_{\rm ped} < 0.3$ H-modes with discrete ELMs and low D_α were seen on C-Mod. However, ELMs also occurred on C-Mod at higher ν^* and lower β, a parameter range which was not accessed in the JFT-2M comparison discharges at constant $P_{\rm NBI}$.

Differences were found in the details of edge fluctuations in the HRS and EDA regimes. In particular, the frequency of the HF mode on JFT-2M was higher (340 kHz) than that of the QC mode in corresponding C-Mod discharges (134 kHz); this is opposite to what might be expected from dimensionless considerations. The C-Mod QC mode has significantly shorter wavelength ($k_{\theta,\rm mid} \sim 2\,{\rm cm}^{-1}$) and higher mode numbers ($n \sim 22$, $m \sim 130$) than the HF mode on JFT-2M ($n \sim 7$, $m \sim 28$). The reasons for these differences in fluctuation characteristics are not currently understood. They presumably reflect conditions which were not matched in this comparison, such as the aspect ratio, the heating technique or the plasma toroidal rotation, which is significant in C-Mod H-modes despite the lack of external momentum input [19] but was low in these JFT-2M plasmas. It is also possible that higher k fluctuation components exist on JFT-2M which were not resolved by the available diagnostics; wall mounted magnetic coils, as shown on C-Mod, are less sensitive to higher k modes [8, 9].

It should be noted that the C-Mod, H-mode observations reported here differ in several respects from those found in more typical shapes with higher elongation. Quasicoherent fluctuations in EDA exhibited two components, with the second component having half the frequency (67 kHz) and wavenumber ($1\,{\rm cm}^{-1}$) of the usually observed QC mode. The lower frequency component is closer in m to, though still higher than, that on JFT-2M. ELMs occurred much more readily in the high triangularity JFT-2M shape indicating differences in edge stability. This will be exploited to further study ELM dynamics and scalings on C-Mod. Prior C-Mod studies have also found somewhat different access conditions for the H-Mode regimes, with more overlap in ν^* between EDA and EDA + ELM regimes; the conditions are clearly complex and cannot be simply expressed in 2-D parameter spaces [2, 10, 16]. These differences, many of which are unexpected, illustrated the importance of conducting dedicated inter-machine comparison experiments to reduce to the extent possible the complicating effects of differences in shape as well as in the dimensionless plasma parameters typically accessed on various tokamaks. Such experiments help to reveal the underlying physics and unify to some extent the observations of many interesting small ELM H-Mode regimes.

Based on the results of this comparison, the regime of small ELMs and high recycling found on both C-Mod and JFT-2M appears potentially interesting for burning plasma experiments. It has been extended to moderate collisionality and has β comparable to Type I ELM regimes. It is not clear from these experiments, which were limited in power, what represents its ultimate pressure limit. This regime may well be connected to 'Type II' ELMs reported on several tokamaks, and possibly to Type V ELMs on NSTX [20], motivating further comparisons.

Acknowledgments

This work was supported by the US Department of Energy, grants DE-FC02-99ER54512 and DE-FG03-96ER54373 and by the Japan Atomic Energy Research Institute. The

encouragement of these experiments by the ITPA Pedestal topical group is gratefully acknowledged.

References

[1] Loarte A *et al* 2004 *Phys. Plasmas* **11** 2668
[2] Oyama N *et al* 2006 *Plasma Phys. Control. Fusion* **48** A171–81
[3] Greenwald M *et al* 1997 *Nucl. Fusion* **37** 793
[4] Kamiya K *et al* 2003 *Nucl. Fusion* **43** 1214
[5] ITER Physics Expert Groups on Confinement and Transport and Confinement Modelling and Database 1999 *Nucl. Fusion* **39** 2175
[6] Greenwald M *et al* 2000 *Plasma Phys. Control. Fusion* **42** A263
[7] Mazurenko A *et al* 2002 *Phys. Rev. Lett.* **89** 225004-1
[8] Hubbard A E *et al* 2001 *Phys. Plasmas* **8** 2033
[9] Snipes J A *et al* 2001 *Plasma Phys. Control. Fusion* **43** L23
[10] Mossessian D *et al* 2003 *Phys. Plasmas* **10** 172
[11] Yushmanov P *et al* 1997 *Nucl. Fusion* **39** B115
[12] Kamiya K *et al* 2004 *Plasma Phys. Control. Fusion* **46** A157
[13] Nagashima N *et al* 2004 *Plasma Phys. Control. Fusion* **46** A381
[14] Kamiya K, Oyama N, Miura Y and Hubbard A E 2004 *Plasma Phys. Control. Fusion* **46** 1745
[15] Lipschultz B *et al* 2006 Operation of Alcator C-Mod with high Z plasma facing components and implications *Phys. Plasmas* **13** at press
[16] Hughes J W *et al* 2002 *Phys. Plasmas* **9** 3019
[17] Terry J L *et al* 2005 *Bull. Am. Phys. Soc.* **50** 318
[18] Porkolab M *et al* 2003 *15th Topical Conf. on Radio Frequency Power in Plasmas (Moran, Wyoming, USA, 2003) AIP Proc.* **294** 162
[19] Rice J *et al* 2004 *Phys. Plasmas* **11** 2427
[20] Maingi R *et al* 2004 *Proc. 31st EPS Conf. on Plasma Physics (London, June–July 2004)* vol 28B, P-2.189